Inorg. Chem. **2004**, *43*, 430–435

Hybrid Cluster-Cages Formed via Cyanometalate Condensation: $Cs\subset Co_4Ru_6S_2(CN)_{12}$, $Co_4Ru_9S_6(CN)_9$, and $Rh_4Ru_9S_6(CN)_9$ Frameworks

Matthew L. Kuhlman and Thomas B. Rauchfuss*

Department of Chemistry, University of Illinois at Urbana−Champaign, Urbana, Illinois 61801

Received June 30, 2003

Condensation of cyanometalates and cluster building blocks leads to the formation of hybrid molecular cyanometalate cages. Specifically, the reaction of $\{Cs\subset[CpCo(CN)_3]_4[Cp^*Ru]_3\}$ and $[(cymene)_2Ru_3S_2(NCMe)_3]PF_6$ produced $\{Cs\subset[CpCo(CN)_3]_4[(cymene)_2Ru_3S_2][Cp^*Ru]_3\}(PF_6)_2$, $\mathbf{Cs\subset Co_4Ru_6S_2^{2+}}$. Single-crystal X-ray diffraction, NMR spectroscopy, and ESI-MS measurements show that $\mathbf{Cs\subset Co_4Ru_6S_2^{2+}}$ consists of a $Ru_4Co_4(CN)_{12}$ box fused with a Ru_3S_2 cluster via a common Ru atom. The reaction of $PPN[CpCo(CN)_3]$ and 0.75 equiv of $[(cymene)_2(MeCN)_3Ru_3S_2](PF_6)_2$ in MeCN solution produced $\{[CpCo(CN)_3]_4[(cymene)_2Ru_3S_2]_3\}(PF_6)_2$, $\mathbf{Co_4Ru_9S_6^{2+}}$. Crystallographic analysis, together with NMR and ESI-MS measurements, shows that $\mathbf{Co_4Ru_9S_6^{2+}}$ consists of a $Ru_3Co_4(CN)_9$ "defect box" core, wherein each Ru is fused to a Ru_3S_2 clusters. The analogous condensation using $[Cp^*Rh(CN)_3]^-$ in place of $[CpCo(CN)_3]^-$ produced the related cluster-cage $\mathbf{Rh_4Ru_9S_6^{2+}}$. Electrochemical analyses of both $\mathbf{Co_4Ru_9S_6^{2+}}$ and $\mathbf{Rh_4Ru_9S_6^{2+}}$ can be rationalized in the context of reduction at the cluster and the Co^{III} subunits, the latter being affected by the presence of alkali metal cations.

Introduction

Cyanometalates have been widely employed as building blocks for the construction of multimetallic arrays, with recent emphasis on magnetic solids[1] and molecular cages exhibiting host−guest behavior.[2] We have studied the reaction of $[CpCo(CN)_3]^-$ with CpM^{n+} sources to generate boxes[3], defect boxes, and double boxes.[4] These condensations are highly efficient, and the flexibility of the syntheses allows one to fine-tune the associated host−guest behavior.[2,5]

The idea of using metal clusters as building blocks in the condensation-syntheses of metal cyanide cages and solids has been developed by Fedorov,[6,7] Long, Fedin and their co-workers. For example, Long et al. demonstrated the condensation of cyanide-substituted Chevrel clusters and metal cations, M^{z+}, to afford expanded Prussian blue frameworks, which exhibit host−guest behavior (Figure 1).[8,9] Fedin and co-workers condensed cyanide-substituted cubane clusters and M^{z+} to generate cubic frameworks possessing cavities with void volumes of 1664 Å^3 (Figure 1).[10,11] Condensation of incomplete cubanes has resulted in high-nuclearity cage-clusters, some of which exhibit catalytic activity.[12−17]

In view of these promising precedents, we initiated a project aimed at generating cyanometalate cages using organometallic clusters as building blocks. To avoid three-

* Author to whom correspondence should be addressed. E-mail address: rauchfuz@uiuc.edu.

(1) Beauvais, L. G.; Long, J. R. *J. Am. Chem. Soc.* **2002**, *124*, 12096−12097.
(2) Hsu, S. C. N.; Ramesh, M.; Espenson, J. H.; Rauchfuss, T. B. *Angew. Chem., Int. Ed.* **2003**, *42*, 2663−2666.
(3) Klausmeyer, K. K.; Wilson, S. R.; Rauchfuss, T. B. *J. Am. Chem. Soc.* **1999**, *121*, 2705−2711.
(4) Contakes, S. M.; Kuhlman, M. L.; Ramesh, M.; Wilson, S. R.; Rauchfuss, T. B. *Proc. Natl. Acad. Sci. U.S.A.* **2002**, *99*, 4889−4893.
(5) Kuhlman, M. L.; Rauchfuss, T. B. *J. Am. Chem. Soc.* **2003**, *125*, 10084−10092.
(6) Naumov, N. G.; Virovets, A. V.; Mironov, Y. I.; Artemkina, S. B.; Fedorov, V. E. *Ukr. Khim. Zh. (Russ. Ed.)* **1999**, *65*, 21−27.
(7) Naumov, N. G.; Virovets, A. V.; Fedorov, V. E. *Inorg. Chem. Commun.* **2000**, *3*, 71−72.
(8) Beauvais, L. G.; Shores, M. P.; Long, J. R. *Chem. Mater.* **1998**, *10*, 3783−3786.
(9) Beauvais, L. G.; Shores, M. P.; Long, J. R. *J. Am. Chem. Soc.* **2000**, *122*, 2763−2772.
(10) Fedin, V. P.; Kalinina, I. V.; Virovets, A. V.; Fenske, D. *Russ. Chem. Bull.* **2001**, *50*, 1525−1528.
(11) Fedin, V. P.; Virovets, A. V.; Kalinina, I. V.; Ikorskii, V. N.; Elsegood, M. R. J.; Clegg, W. *Eur. J. Inorg. Chem.* **2000**, 2341−2343.
(12) Seino, H.; Kaneko, T.; Fujii, S.; Hidai, M.; Mizobe, Y. *Inorg. Chem.* ACS ASAP.
(13) Takei, I.; Suzuki, K.; Enta, Y.; Dohki, K.; Suzuki, T.; Mizobe, Y.; Hidai, M. *Organometallics* **2003**, *22*, 1790−1792.
(14) Herbst, K.; Zanello, P.; Corsini, M.; D'Amelio, N.; Dahlenburg, L.; Brorson, M. *Inorg. Chem.* **2003**, *42*, 974−981.
(15) Herbst, K.; Monari, M.; Brorson, M. *Inorg. Chem.* **2001**, *40*, 2979−2985.
(16) Takagi, F.; Seino, H.; Mizobe, Y.; Hidai, M. *Organometallics* **2002**, *21*, 694−699.
(17) Sakane, G.; Kawasaki, H.; Oomori, T.; Yamasaki, M.; Adachi, H.; Shibahara, T. *J. Cluster Sci.* **2002**, *13*, 75−102.

10.1021/ic034745s CCC: $27.50 © 2004 American Chemical Society
Published on Web 12/18/2003

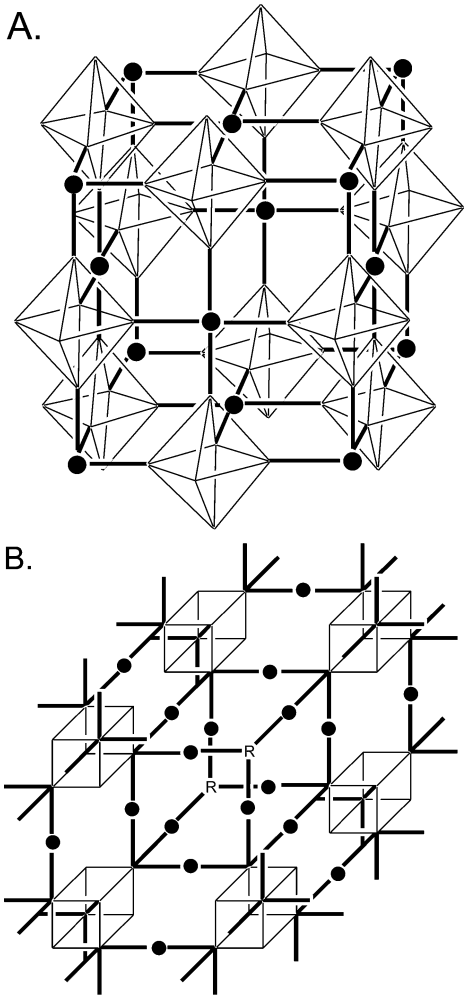

Figure 1. (A) Expanded Prussian blue framework from cyanide substituted Chevrel clusters, $[Re_6Se_8(CN)_6]^{4-}$, and Fe^{3+} (●). (B) Expanded cubic framework from cyanide substituted cubane clusters, $[W_4Te_4(CN)_{12}]^{6-}$, and Co^{2+} (●). The cyanide ligands are represented by bold lines, and R = cubane cluster. The selenium atoms for the Chevrel clusters and all H_2O molecules have been omitted for clarity.

dimensional solids, clusters consisting of only one labile vertex were utilized. We anticipated that incorporation of metal sulfido clusters within a cyanometalate cage may ultimately confer unique redox activity (associated with the cluster vertices) that in turn could allow us to control host−guest behavior. One can envision two basic approaches to cyano-cluster-cage hybrids depending on whether the cluster is the Lewis acid (cyanometalate acceptor) or Lewis base (cyanometalate). The two routes are (A) $E_x[ML_y]_z[M(CN)_3]$ + *fac*-$[L_3M(NCMe)_3]^{n+}$ and (B) *fac*-$L_3M(CN)_3$ + $[ML_y]_zE_x$-$[M(NCMe)_3]$ (Scheme 1, where E is a main group linker atom).

One basic problem with the cluster condensation approaches, at least when the targets are molecular products, is the scarcity of site-differentiated clusters with the appropriate tritopic sites. The recently described $[(cymene)_2Ru_3S_2(NCMe)_3]^{2+}$ represents a rare example of such a site-differentiated cluster. This species arises from the photolysis of MeCN solutions of $[(cymene)_3Ru_3S_2]^{2+}$, which is easily prepared. Although $[(cymene)_2Ru_3S_2(NCMe)_3]^{2+}$ has never been isolated, and in fact appears to be unstable, it forms stable derivatives with PPh_3 and 9-ane-S3.[18]

Scheme 1

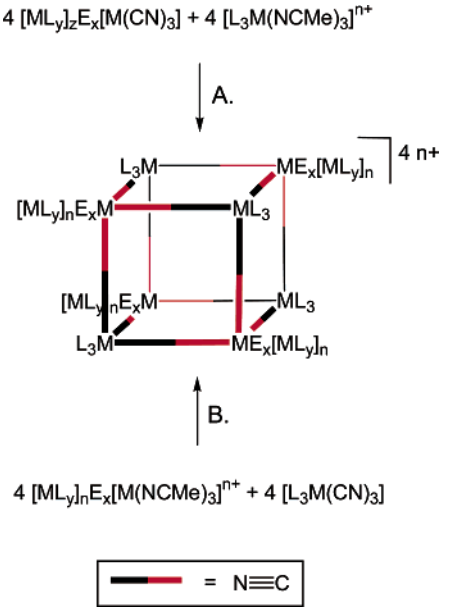

This paper describes two approaches to cluster cages. First, we describe the interaction of the Ru_3 cluster with $\{Cs\subset[CpCo(CN)_3]_4[Cp^*Ru]_3\}$. We had previously demonstrated that this cyanometalate cage functions as a facial (tridentate) metalloligand, evidenced by its formation of strong complexes with metal cations such as Cp^*Rh^{2+} and Fe^{2+} to give box-like and double-box-like cages, respectively.[4] In the second approach, $[(cymene)_2Ru_3S_2(NCMe)_3]^{2+}$ was simply employed as the equivalent to $[Cp^*Rh(NCMe)_3]^{2+}$ in its condensation with $[(C_5R_5)M(CN)_3]^-$. The latter reaction is precedented by the condensation routes to give the "defect boxes" $[Cp^*_7Rh_7(CN)_{12}]^{2+}$ and $[Cp_4Cp^*_3Co_4Rh_3(CN)_{12}]^{2+}$.[3,19]

Results and Discussion

Synthesis and Characterization of $\{Cs\subset[CpCo(CN)_3]_4[(cymene)_2Ru_3S_2][Cp^*Ru]_3\}^{2+}$. The photochemical synthesis of $[(cymene)_2Ru_3S_2(NCMe)_3]^{2+}$ in the presence of $\{Cs\subset[CpCo(CN)_3]_4[Cp^*Ru]_3\}$ produced a good yield of the targeted cluster-cage $\{Cs\subset[CpCo(CN)_3]_4[Cp^*Ru]_3[(cymene)_2Ru_3S_2]\}^{2+}$, $\mathbf{Cs\subset Co_4Ru_6S_2}^{2+}$(Scheme 2). The IR spectrum of the cluster-cage features ν_{CN} at 2154 cm^{-1}, is shifted to a higher energy relative to the ν_{CNt} band (2124 cm^{-1}) for $\mathbf{Cs\subset Co_4Ru_3}$ (Figure 2). The ^1H NMR and ESI-MS spectra confirmed the symmetry and stoichiometry of the cation.

Single-crystal X-ray crystallography confirmed the general structure of the hybrid cluster-box with C_s symmetry (Figure 3). The bond distances and angles of the box resemble those for the parent $\{Cs\subset[CpCo(CN)_3]_4[Cp^*Ru]_3\}$.[5] The cluster subunit also closely resembles the structures for isolated $[(cymene)_3Ru_3S_2]^{2+}$ and $[(cymene)_2Ru_3S_2(NCMe)_2(PPh_3)]^{2+}$.[18,20]

(18) Eckermann, A. L.; Fenske, D.; Rauchfuss, T. B. *Inorg. Chem.* **2001**, *40*, 1459−1465.
(19) Contakes, S. M.; Klausmeyer, K. K.; Milberg, R. M.; Wilson, S. R.; Rauchfuss, T. B. *Organometallics* **1998**, *17*, 3633−3635.

Scheme 2

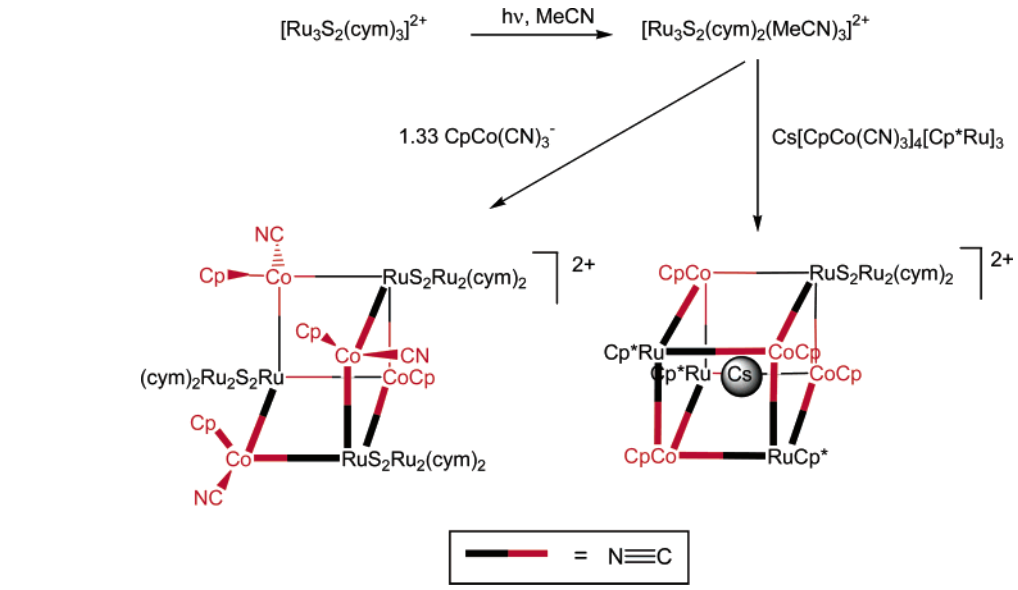

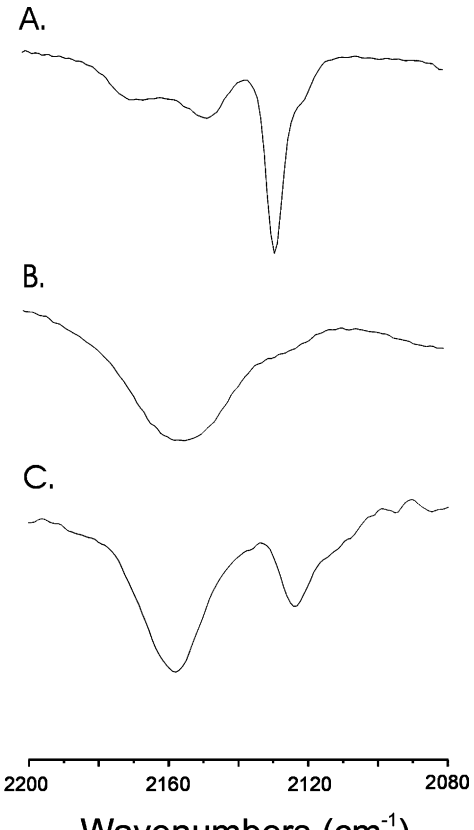

Figure 2. IR spectra (MeCN) in the ν_{CN} region for **Cs⊂Co₄Ru₃** (A), **Cs⊂Co₄Ru₆S₂**$^{2+}$ (B), and **Co₄Ru₉S₆**$^{2+}$(C).

The lowered symmetry for the cluster environment is manifested in the distortion of the Ru_3 framework such that one Ru−Ru bond is 0.1 Å shorter than the other two (Tables 1 and 2). Visual inspection of a space-filling model suggests that the cymene ligands are not sterically prevented from free rotation by adjacent Cp ligands.

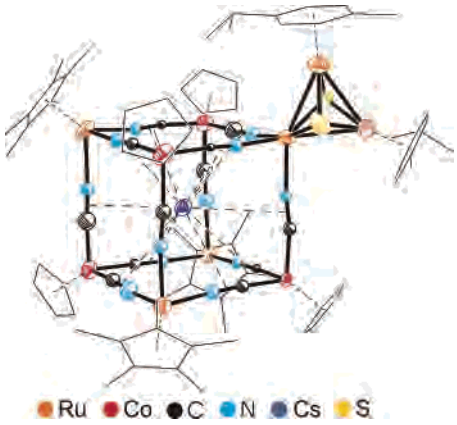

Figure 3. Structure of the dicationic cluster-cage in {Cs⊂[CpCo(CN)$_3$]$_4$-[Cp*Ru]$_3$[(cymene)$_2$Ru$_3$S$_2$]}(PF$_6$)$_2$. Thermal ellipsoids are drawn at the 50% level.

The Cs atom is unsymmetrically situated with respect to the eight vertexes of the box: Cp*Ru···Cs = 4.429 Å (av), (cym)$_2$Ru$_2$S$_2$Ru···Cs = 4.594 Å, CpCo···Cs = 4.401 Å (av), and $CpCo_{unique}$···Cs = 4.326 Å. The Cs atom is repelled from the dicationic (cym)$_2$S$_2$Ru$_3^{2+}$ cluster toward the unique CpCo(CN)$_3^-$ fragment trans to the cluster. The fact that Cs$^+$ remains bound within the receptor's cationic framework demonstrate the strength of Cs$^+$ interaction with the cyanide π electron density.

Synthesis and Characterization of [CpCo(CN)$_3$]$_4$-[(cymene)$_2$Ru$_3$S$_2$]$_3$(PF$_6$)$_2$. The synthesis of **Cs⊂Co₄Ru₆S₂**$^{2+}$ demonstrated that [(cymene)$_2$Ru$_3$S$_2$(NCMe)$_3$]$^{2+}$ can serve as a tritopic Lewis acid. To extend this concept, we treated [(cymene)$_2$Ru$_3$S$_2$(NCMe)$_3$]$^{2+}$ with 1.33 equiv of [CpCo(CN)$_3$]$^-$. NMR analysis showed that this reaction produced the symmetric triple cluster derivative {[CpCo(CN)$_3$]$_4$[(cymene)$_2$-Ru$_3$S$_2$]$_3$}$^{2+}$, **Co₄Ru₉S₆**$^{2+}$ (Scheme 2). The ^{1}H NMR spectrum of **Co₄Ru₉S₆**$^{2+}$ consists of a 1:3 pattern in the Cp region, consistent with C_{3v} symmetry. The ^{1}H NMR spectrum also confirmed the ratio of six cymene ligands to four Cp ligands with the cymene ligands being chemically equivalent. The reaction stoichiometry is not critical: with increased amounts

(20) Lockemeyer, J. R.; Rauchfuss, T. B.; Rheingold, A. L. *J. Am. Chem. Soc.* **1989**, *111*, 5733−5738.

Table 1. Crystallographic Data for $\{Cs\subset[CpCo(CN)_3]_4[Cp^*Ru]_3[(cymene)_2Ru_3S_2]\}(PF_6)_2$

empirical formula	$C_{92}H_{108}Co_4CsF_{12}N_{17}P_2Ru_6S_2$
fw	2781.06
space group	$P\bar{1}$
crystal size (mm^3)	0.24 × 0.07 × 0.02
temp (K)	193(2)
λ (Å)	0.71073
a (Å)	15.586(4)
b (Å)	26.955(8)
c (Å)	28.378(8)
α (deg)	111.742(6)
β (deg)	91.535(7)
γ (deg)	93.373(6)
V (Å^3)	11039(5)
Z	4
$\rho_{calc\ mg/m^3}$	1.673
μ(Mo Kα, mm^{-1})	1.841
min and max transmn	0.7666/0.9646
reflns measd/indep	45846/15947
data/restraints/params	13345/894/777
F(000)	5504
GOF	0.827
R_{int}	0.0680
R1 [$I > 2\sigma$] (all data)[a]	0.0821 (0.2138)
wR2 [$I > 2\sigma$] (all data)[b]	0.1596 (0.1944)
max peak/hole (e^-/Å^3)	0.743/−0.748

[a] $R1 = \sum||F_o| - |F_c||/\sum|F_o|$. [b] $wR2 = \{\sum[w(F_o^2 - F_c^2)^2]/\sum[w(F_o^2)^2]\}^{1/2}$.

Table 2. Selected Bond Distances (Å) and Angles (deg) for $\{Cs\subset[CpCo(CN)_3]_4[Cp^*Ru]_3[(cymene)_2Ru_3S_2]\}\{PF_6\}_2$

Ru(4)−Ru(5)	2.831	Ru(5)−Ru(4)−Ru(6)	57.75
Ru(4)−Ru(6)	2.823	Ru(4)−Ru(6)−Ru(5)	61.27
Ru(5)−Ru(6)	2.731	Ru(6)−Ru(5)−Ru(4)	60.98
Ru(4)−N(5)	2.126	N(5)−Ru(4)−N(8)	91.03
Ru(4)−N(8)	2.088	N(8)−Ru(4)−N(12)	84.65
Ru(4)−N(12)	2.122	N(5)−Ru(4)−N(12)	85.80
Ru(4)−S(1)	2.231	S(1)−Ru(4)−S(2)	89.02
Ru(5)−S(1)	2.234	S(1)−Ru(5)−S(2)	88.83
Ru(6)−S(1)	2.257	S(1)−Ru(6)−S(2)	87.90
Co(1)−C(1)	1.900	C(1)−Co(5)−C(2)	90.78
Co(1)−C(2)	1.816		
Ru(1)−N(2)	2.122	N(2)−Ru(7)−N(7)	88.87
Ru(1)−N(7)	2.068		
C(1)−N(1)	1.179	N(1)−C(1)−Co(1)	169.82
Cs(1)−N(1)	3.543		
Cs(1)−C(1)	3.682		

of $\mathbf{Ru_3S_2}$, one observes only the defect box and unreacted $\mathbf{Ru_3S_2}$. Similarly, at low $[\mathbf{Ru_3S_2}]/[CpCo(CN)_3]^-$ one still observes $\mathbf{Co_4Ru_9S_6}^{2+}$ together with unreacted $[CpCo(CN)_3]^-$ (Figure 4).

The IR spectrum of $\mathbf{Co_4Ru_9S_6}^{2+}$ features ν_{CN} at 2156 and 2124 cm^{-1}, with the higher energy band assigned to $\nu_{(\mu-CN)}$. This band is shifted by 35 cm^{-1} to higher frequency relative to [K-18-crown-6][$CpCo(CN)_3$].[21] The band at 2124 cm^{-1} is assigned to ν_{CNt}, as seen for $\mathbf{Cs\subset Co_4Ru_3}$ (Figure 2). The formula for $\mathbf{Co_4Ru_9S_6}^{2+}$ was also confirmed by ESI-MS with M^{2+} at m/z = 1358. X-ray crystallography confirmed the structure of the cage, which has idealized C_{3v} symmetry (Figure 5). The three terminal cyanide ligands are oriented away from the open vertex, as seen in other cationic defect boxes.[3,19] Although the X-ray data allowed us to determine the metal framework, the data was not sufficient to support further refinement.

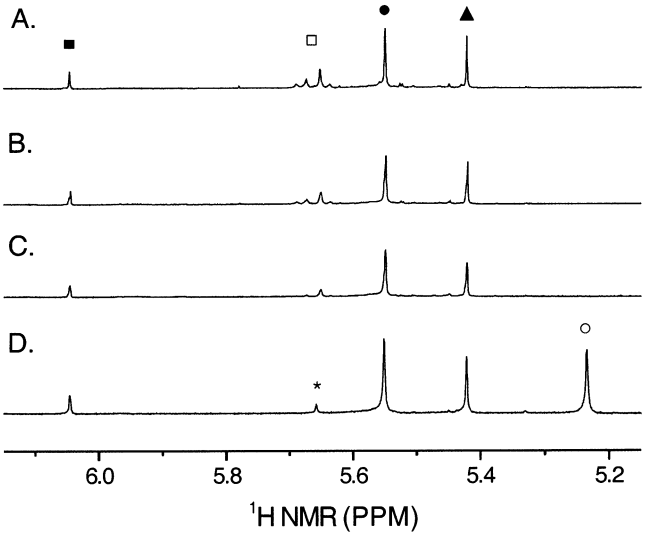

Figure 4. 500 MHz ^{1}H NMR spectra for the reaction of $[CpCo(CN)_3]^-$ and $[(cymene)_2Ru_3S_2(MeCN)_3]^{2+}$ at various ratios. The reactions were performed in sealed NMR tubes in CD_3CN solution, which were irradiated for 3 h and then immediately analyzed: (A) 4:5 ratio of $[CpCo(CN)_3]^-$:$[(cymene)_2Ru_3S_2(MeCN)_3]^{2+}$, (B) 4:4 ratio of $[CpCo(CN)_3]^-$:$[(cymene)_2Ru_3S_2(MeCN)_3]^{2+}$, (C) 4:3 ratio of $[CpCo(CN)_3]^-$:$[(cymene)_2Ru_3S_2(MeCN)_3]^{2+}$, (D) 7:3 ratio of $[CpCo(CN)_3]^-$:$[(cymene)_2Ru_3S_2(MeCN)_3]^{2+}$. ■ = Cp for unique CpCo of $\mathbf{Co_4Ru_9S_6}^{2+}$. □ = aromatic cymene region for $[(cymene)_2Ru_3S_2(MeCN)_3]^{2+}$. ● = aromatic cymene region for $\mathbf{Co_4Ru_9S_6}^{2+}$. ▲ = Cp for three equiv CpCo of $\mathbf{Co_4Ru_9S_6}^{2+}$. ○ = Cp for $[CpCo(CN)_3]^-$. ∗ = impurity.

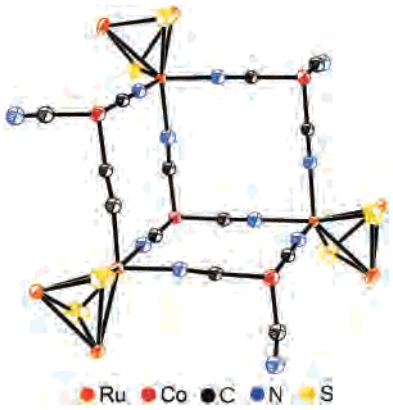

Figure 5. Structure of the dicationic cluster-cage in $\{[CpCo(CN)_3]_4[(cymene)_2Ru_3S_2]_3\}(PF_6)_2$; the hydrocarbon ligands are omitted for clarity. Thermal ellipsoids are drawn at the 25% level.

Synthesis and Characterization of $[Cp^*Rh(CN)_3]_4[(cymene)_2Ru_3S_2]_3(PF_6)_2$. The Cp*Rh-containing analogue of $\mathbf{Co_4Ru_9S_6}^{2+}$ was synthesized from $[(cymene)_2Ru_3S_2(NCMe)_3]^{2+}$ and 1.33 equiv of $[Cp^*Rh(CN)_3]^-$. The IR spectrum of this species features ν_{CN} at 2155 and 2118 cm^{-1}, vs 2123 and 2118 cm^{-1} for $Et_4N[Cp^*Rh(CN)_3]$.[22] The formula $\{[Cp^*Rh(CN)_3]_4[(cymene)_2Ru_3S_2]_3\}^{2+}$, $\mathbf{Rh_4Ru_9S_6}^{2+}$, was also confirmed by ESI-MS with M^{2+} at m/z = 1587. The ^{1}H NMR spectrum of $\mathbf{Rh_4Ru_9S_6}^{2+}$ revealed a 1:3 pattern in the Cp* region, consistent with C_{3v} symmetry. The same spectrum also confirmed (i) the cymene/Cp* ratio of 6/4 and (ii) the chemical equivalency of the six cymene ligands.

(21) Dineen, J. A.; Pauson, P. L. *J. Organomet. Chem.* **1972**, *43*, 209−212.

(22) Klausmeyer, K. K.; Rauchfuss, T. B.; Wilson, S. R. *Angew. Chem., Int. Ed.* **1998**, *37*, 1694−1696.

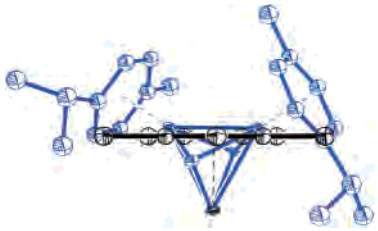

Figure 6. Overlay of the tritopic Lewis acids: $(cymene)_2Ru_2S_2Ru^{2+}$ and Cp^*Ru^+ with coordinates taken from the crystallographically determined structure of $\{Cs\subset[CpCo(CN)_3]_4[Cp^*Ru]_3[(cymene)_2Ru_3S_2]\}(PF_6)_2$. The metal atoms are superimposed.

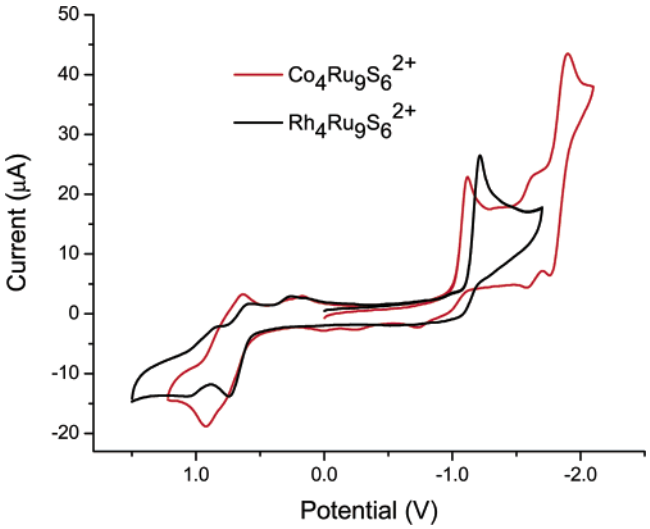

Figure 7. Cyclic voltammograms of $\mathbf{Co_4Ru_9S_6^{2+}}$ and $\mathbf{Rh_4Ru_9S_6^{2+}}$.

As in the previous case of $\mathbf{Co_4Ru_9S_6^{2+}}$ the stoichiometry of reaction is not critical. In both the CpCo and Cp*Rh cases, we were unable to generate completed cluster boxes. Previous worked has shown that the steric hindrance imposed by large facially capping ligands such as Cp* can prevent box completion.[19] In terms of steric-profile, the "ligand" $(cymene)_2Ru_2S_2$ is larger than Cp* as indicated by visual inspection although the orientational asymmetry of the cymene ligand complicates the comparison (Figure 6).

Electrochemical Analysis of $Co_4Ru_9S_6^{2+}$ and $Rh_4Ru_9S_6^{2+}$. Cyclic voltammetry provided insights into the redox responsiveness of the various subunits of the cluster-cages $\mathbf{Co_4Ru_9S_6^{2+}}$ and $\mathbf{Rh_4Ru_9S_6^{2+}}$. Both undergo an irreversible reduction at ca. −1.2 V, which is assigned to the reduction of the Ru_3S_2 subunits. At more extreme potentials, $\mathbf{Co_4Ru_9S_6^{2+}}$ undergoes two reversible reductions, assigned to $Co^{III/II}$. In contrast $\mathbf{Rh_4Ru_9S_6^{2+}}$ shows only the ∼−1.2 V reductions, the $Cp^*Rh^{III}(CN)_3$ units apparently being more difficult to reduce than $[CpCo(CN)_3]^-$ (Figure 7). Both $\mathbf{Co_4Ru_9S_6^{2+}}$ and $\mathbf{Rh_4Ru_9S_6^{2+}}$ undergo two irreversible oxidations at ca. 0.7 and 0.9 V, assigned to the oxidation of the Ru_3S_2 subunits. Other aspects of the redox properties are presented in the Experimental Section.

In the presence of Cs^+, the two Co-centered reductions of $\mathbf{Co_4Ru_9S_6^{2+}}$ shift positively by 400 and 100 mV. The same effect was also observed upon addition of K^+ and Na^+ salts. The fact that all three cations elicited the same effect suggests that these cations interact similarly with the cluster-cage, probably via binding to the terminal cyanide ligands. Titration of $\mathbf{Co_4Ru_9S_6^{2+}}$ with Cs^+ revealed that redox couples shift for <3 equiv of cation but not with additional equivalents (Figure 8).

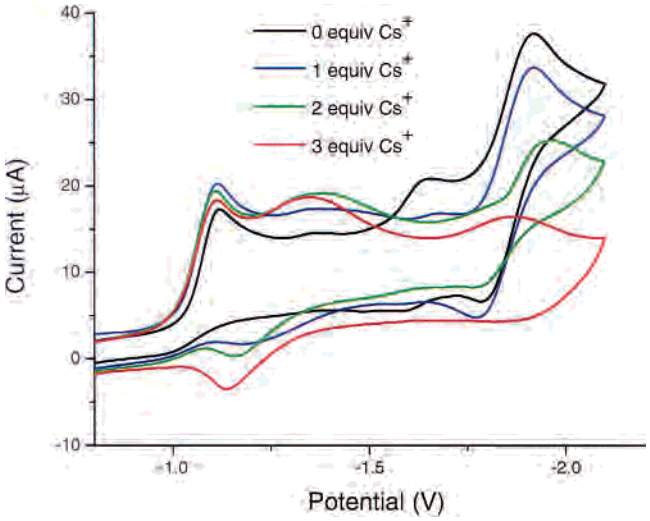

Figure 8. Cyclic voltammograms of $\mathbf{Co_4Ru_9S_6^{2+}}$ upon treatment with 0, 1, 2, and 3 equiv of Cs^+ (scan rate of 50 mV/s on 10^{-3} M MeCN solutions in 0.01 M Bu_4NPF_6). Equivalents of Cs^+ were added as a 0.005 M CsOTf solution.

Conclusions

Molecular cyanometalate cages are generally prepared by the condensation of tritopic Lewis acids and facial tricyanometalates. In this study we demonstrate that Lewis acidic clusters also participate in the condensation. In this way we generated some relatively high nuclearity molecular species, i.e., those with Co_4Ru_9 and Rh_4Ru_9 frameworks. The steric bulk of the $(cymene)_2Ru_3S_2$ vertex precludes, however, formation of completed boxes $M_4[Ru_3S_2]_4$.

Fujita and co-workers have encapsulated an ion-pair within a cationic receptor,[23] whereas we have encapsulated a cation in a cationic receptor. $\mathbf{Cs\subset Co_4Ru_6S_2^{2+}}$ is a rare structurally characterized cationic receptor bearing a cationic guest molecule. Ordinarily one would expect that cationic receptors would repel other cations. The stability of this species indicates the ability of the cluster to localize the positive charge, thereby reducing Coulombic repulsions between the cationic cage vertices and Cs^+. Efforts to extend the inclusion chemistry of alkali metals were unsuccessful. Reduction of the cluster-cage $\mathbf{Co_4Ru_9S_6^{2+}}$ in the presence of alkali metal cations did not lead to inclusion complexes.

Aside from $[(cym)_2Ru_3S_2(NCMe)_3]^{2+}$, few metal clusters with triple Lewis acid sites are known. The absence of site-differentiated cluster compounds remains an important gap in the palette of metal cluster chemistry.

Materials and Methods

General. Standard Schlenck techniques were used in all syntheses. The precursors $Et_4N[Cp^*Rh(CN_3)]$,[22] $[(cymene)_3Ru_3S_2](PF_6)_2$,[20] and $\{Cs[CpCo(CN)_3]_4[Cp^*Ru]_3\}$[4] were prepared according

(23) Bourgeois, J.-P.; Fujita, M.; Kawano, M.; Sakamoto, S.; Yamaguchi, K. *J. Am. Chem. Soc.* **2003**, *125*, 9260−9261.

to published procedures. An immersion reactor (150 mL) with a water-cooled quartz sheath was used for photolyses. The UV light source was a high-pressure mercury-vapor lamp (Hanovia, 450 W). ^{13}C and ^{1}H NMR spectra were acquired on Unity Varian 400 and 500 spectrometers. Electrochemical experiments were done on a BAS-100 electrochemical analyzer. Cyclic voltammograms were measured at a scan rate of 50 mV/s on 10^{-3} M MeCN solutions using 0.01 M Bu_4NPF_6 as a supporting electrolyte and referenced to internal $Cp_2Fe^{+/0}$. A platinum wire counter electrode, a glassy carbon working electrode, and a Ag/AgCl reference electrode were used. Elemental analyses were done by the Microanalytical Laboratory in the School of Chemical Sciences.

Improved Synthesis of $NH_4[CpCo(CN)_3]$. A slurry of 8.0 g (19.7 mmol) of $CpCo(CO)I_2$ in 50 mL of MeOH was added to a solution of 4.0 g (61 mmol) of KCN in 100 mL of MeOH, and the resulting solution was heated at reflux for 48 h. The reaction mixture was allowed to cool and then filtered in air. The brown-colored filtrate was evaporated to dryness, and the residue was washed twice with 50 mL of MeCN to remove a dark brown impurity. The remaining yellow powder was dissolved in 1 L of hot MeCN to give a clear yellow solution. A solution of 5 g (30 mmol) of NH_4PF_6 in 50 mL of MeCN was then added to the yellow solution to precipitate yellow $NH_4[CpCo(CN)_3]$. Yield: 2.5 g (58%). A solution of 0.5 g (2.28 mmol) of $NH_4[CpCo(CN)_3]$ in 20 mL of H_2O was added to a solution of 1.4 g (2.44 mmol) of PPNCl in 500 mL of H_2O. Yellow-orange microcrystals of $PPN[CpCo(CN)_3]\cdot H_2O$ immediately precipitated. This crude product was purified by extraction into 20 mL of MeCN followed by the addition of 100 mL of Et_2O. The product was collected by filtration, washed with 20 mL of Et_2O, and dried under vacuum. Yield: 1.62 g (96%). Anal. Calcd for $C_{44}H_{37}N_4CoOP_2$ (found): C, 69.66 (69.31); H, 4.92 (4.64); N, 7.38 (7.88).

$\{Cs[CpCo(CN)_3]_4[Cp^*Ru]_3[(cymene)_2Ru_3S_2]\}(PF_6)_2$. A solution of 174 mg (0.164 mmol) of $[(cymene)_3Ru_3S_2](PF_6)_2$ in 10 mL of MeCN was added to a solution of 271 mg (0.164 mmol) of $\{Cs[CpCo(CN)_3]_4[Cp^*Ru]_3\}$ in 130 mL of THF. The red solution was irradiated with UV light within the immersion reactor and stirred for 3 h. The solution was evaporated to dryness and then redissolved in 10 mL of MeCN. Addition of 60 mL of Et_2O to the red solution resulted in a red powder, which was collected by filtration and washed with 30 mL of Et_2O. Yield: 378 mg (89%). IR (MeCN, cm^{-1}): $\nu_{CN} = 2154$. ^{1}H NMR (MeCN): 1.407 (d, 12H), 1.685 (s, 45H), 2.509(s, 6H), 2.84 (sept, 2H), 5.523 (m, 8H), 5.597 (s, 5H), 5.618 (s, 15H). ESI-MS: $m/z = 1143.2$ ($[M^{2+}]$). Anal. Calcd for $C_{82}H_{93}N_{12}Co_4CsF_{12}P_2Ru_6S_2$ (found): C, 38.24 (37.66); H, 3.64 (3.65); N, 6.53 (6.42). Crystals of $\{CsCo_4Ru_6S_2\}(PF_6)_2$ were grown by vapor diffusion of Et_2O into a solution of 30 mg of $\{CsCo_4Ru_6S_2\}(PF_6)_2$ in 3 mL of MeCN over the course of 1 week.

$\{[CpCo(CN)_3]_4[(cymene)_2Ru_3S_2]_3\}(PF_6)_2$. A solution of 300 mg (0.283 mmol) of $[(cymene)_3Ru_3S_2](PF_6)_2$ in 70 mL of MeCN was added to a solution of 280 mg (0.377 mmol) of $PPN[CpCo(CN)_3]$ in 80 mL of MeCN. The red solution was photolyzed within the immersion reactor with stirring for 3 h. The solution was evaporated to dryness and then redissolved in 30 mL of MeCN. The addition of 150 mL of Et_2O to the red solution precipitated a red powder, which was collected by filtration and washed with 60 mL of Et_2O. Yield: 260 mg (92%). IR (MeCN, cm^{-1}): $\nu_{CN} = 2156, 2124$. ^{1}H NMR (MeCN): 1.365 (d, 36H), 2.367 (s, 18H), 2.753 (sept, 6H), 5.420 (s, 15H), 5.549 (s, 24H), 6.053 (s, 5H). ESI-MS: $m/z = 1358.0$ ($[M^{2+}]$). Anal. Calcd for $C_{82}H_{93}N_{12}Co_4CsF_{12}P_2Ru_6S_2$ (found): C, 36.76 (36.68); H, 3.49 (3.50); N, 5.59 (5.82). Crystals of $\{Co_4Ru_9S_6\}(PF_6)_2$ grew over the course of 2 weeks by vapor diffusion of Et_2O into a solution of 25 mg of $\{Co_4Ru_9S_6\}(PF_6)_2$ in 3 mL of MeCN over the course of 2 weeks.

$\{[Cp^*Rh(CN)_3]_4[(cymene)_2Ru_3S_2]_3\}(PF_6)_2$. A solution of 126 mg (0.119 mmol) of $[(cymene)_3Ru_3S_2](PF_6)_2$ in 20 mL of MeCN was added to a solution of 74 mg (0.159 mmol) of $Et_4N[Cp^*Rh(CN)_3]$ in 30 mL of MeCN. The red solution was irradiated with UV light within the immersion reactor and stirred for 3 h. The resulting brown solution was evaporated to dryness, and the resulting brown residue was redissolved in 15 mL of MeCN. The addition of 80 mL of Et_2O to the brown solution precipitated a brown powder, which was collected and washed with 30 mL of Et_2O. Yield: 110 mg (80%). IR (MeCN, cm^{-1}): $\nu_{CN} = 2155, 2118$. ^{1}H NMR (MeCN): 1.339 (d, 36H), 1.977 (s, 45H), 2.377 (s, 18H), 2.539 (s, 15H), 2.693 (sept, 6H), 5.469 (s, 24H). ESI-MS: $m/z = 1587.2$ ($[M^{2+}]$). Anal. Calcd for $C_{112}H_{144}N_{12}Rh_4F_{12}P_2Ru_9S_2$ (found): C, 38.86 (38.55); H, 4.19 (4.03); N, 4.86 (4.87).

Crystallography. Crystals were mounted on thin glass fibers using Paratone-N oil (Exxon) before being transferred to a Siemens Platform/CCD automated diffractometer for data collection. Data processing was performed with SAINT PLUS version 6.22. Structures were solved using direct methods and refined using full matrix least squares on F^2 using the program Bruker SHELXTL version 6.10. Hydrogen atoms were fixed in idealized positions with thermal parameters 1.5 times those of the attached carbon atoms. The data were corrected for absorption on the basis of Ψ-scans. Specific details for each crystal are given in Table 2. Full crystallographic details have been deposited with the Cambridge Crystallographic Data Center as supplementary publication numbers CCDC-XXXXX.

Acknowledgment. This research was supported by the Department of Energy. We thank Scott Wilson and Teresa Prussak-Wieckowska for assistance with the X-ray crystallography. We also would like to thank Prof. Dr. Dieter Fenske and Dr. Markus Wunder at the Universität Karlsruhe for helpful discussions and assistance with the X-ray crystallography.

Supporting Information Available: Crystallographic data (CIF format) including experimental details and complete tables of bond distances and angles, atomic coordinates, and anisotropic displacement parameters. Figure 9 containing a cyclic voltammogram of $Rh_4Ru_9S_6^{2+}$. This material is available free of charge via the Internet at http://pubs.acs.org.

IC034745S